Molecular Dissection of Transjunctional Voltage Dependence in the Connexin-32 and Connexin-43 Junctions

Ana Revilla, Carmen Castro, and Luis C. Barrio
Unidad Neurología Experimental-C.S.I.C., Departamento de Investigación, Hospital "Ramón y Cajal," 28034 Madrid, Spain

ABSTRACT Most gap junction channels are sensitive to the voltage difference between the two cellular interiors, termed the *transjunctional voltage* (V_j). In several junctions, the conductance transitions induced by V_j show more than one kinetic component. To elucidate the structural basis of the fast and slow components that characterize the V_j dependence of connexin-32 (Cx32) and connexin-43 (Cx43) junctions, we created deletions of both connexins, where most of the carboxy-terminal (CT) domain was removed. The wild-type and "tailless" mutants were expressed in paired *Xenopus* oocytes, and the macroscopic gating properties were analyzed using the dual voltage clamp technique. Truncation of the CT domain of Cx32 and Cx43 abolished the fast mechanism of conductance transitions and induced novel gating properties largely attributable to the slow mechanism of gating. The formation of hybrid junctions comprising wild-type and truncated hemichannels allowed us to infer that the fast and slow components of gating reside in each hemichannel and that both gates close at a negative V_j on the cytoplasmic side. Thus we conclude that the two kinetic components of V_j-sensitive conductance are a result of the action of two different gating mechanisms. They constitute separate structures in the Cx32 and Cx43 molecules, the CT domain being an integral part of fast V_j gating.

INTRODUCTION

Gap junctions are clusters of intercellular channels that form strongly adherent regions that direct the passage of ions and other small molecules between neighboring cells. The junctional conductance (g_j) is subject to regulation by a number of physiological agents, such as voltage, intracellular pH and calcium, second messengers, or phosphorylation (reviewed in Bruzzone et al., 1996). To date, up to 15 different isotypes of connexins have been cloned so far in rodents, and several homologs have also been identified in other vertebrate species. Each gap junctional channel is a dodecamer of connexins that is formed by the tight docking of two hemichannels that span the plasma membranes of neighboring cells (Makowski et al., 1977). Given this peculiar architecture of gap junction channels, they come under the influence of two types of electrical field, the voltage difference between the two interiors or transjunctional voltage (V_j), and that between the intra- and extracellular spaces or membrane potential (V_m). In vertebrates, there are junctions exclusively sensitive to V_j, whereas others show a combined V_j and V_m dependence (reviewed in Barrio et al., 1999). The dependence of junctional conductance on V_j has been extensively analyzed, and studies have revealed that the conductance of all junctions tested so far is V_j sensitive (reviewed in Bennett and Verselis, 1992; Nicholson et al., 1993; White et al., 1995; Bruzzone et al., 1996). At the macroscopic level, the V_j dependence of most of the different types of homomeric junctions share some features. The g_j is at maximum at $V_j = 0$ and decreases more or less symmetrically at increasing positive and negative polarities of V_j to lower nonzero conductance values (termed *residual conductance*). However, junctions comprising different connexin isoforms and different species have divergent V_j gating properties, varying in their voltage sensitivity, residual conductance, and kinetic properties. Some junctions show symmetrical bell-shaped steady-state g_j/V_j curves with g_j transitions of first-order kinetics, as was initially observed in the junctions of amphibian blastomeres (Harris et al., 1981), and which can be well described at each polarity of V_j by a single Boltzmann relation (Spray et al., 1981). Such a model assumes the existence of one gate in each hemichannel that closes at one polarity of V_j and interacts in series with the gate of the counterpart hemichannel. The appropriateness of this model has been confirmed by the formation of heterotypic channels in which each hemichannel largely retained the properties attributable to its homomeric combinations (e.g., Hennemann et al., 1992; Bruzzone et al., 1993; Moreno et al., 1995; Barrio et al., 1997). Experimental efforts have focused on defining those regions of the connexin molecules that participate in the regulation by V_j. In accordance with the general topology of connexins predicted by hydropathy plots (Bennett et al., 1991), there are nine principal domains: four membrane-spanning regions (M1-M4), two extracellular loops (E1 and E2), a cytoplasmic loop (CL) connecting M2 and M3, and the amino-terminus (NT) and carboxy-terminus (CT) domains in the cytoplasmic side. A point mutation analysis that altered the charged residues of Cx32 and Cx26 at the second amino acid of the NT domain and at the M1/E1 boundary could reverse the gating polarity, and the changes observed can account for the calculated gating charges (Verselis et al., 1994). These data support the idea that an interaction

Received for publication 11 February 1999 and in final form 24 May 1999.
Address reprint requests to Dr. Luis C. Barrio, Departamento de Investigación, Neurología Experimental-C.S.I.C., Hospital "Ramón y Cajal," Carretera de Colmenar km 9, 28034 Madrid, Spain. Tel.: +34-91-336-8320; Fax: +34-91-336-9816; E-mail: luis.c.barrio@hrc.es.

0006-3495/99/09/1374/10 $2.00

between the two regions forms a charged complex that is an integral part of the V_j sensor.

However, several lines of evidence suggest that more than one unique V_j gating component might exist. In many junctions, more than a single exponential was necessary to fit the current decay, indicating that multiple voltage-gated transitions occur in these channels. Moreover, there are junctions that clearly exhibit more than a single range of voltage sensitivities, as seen in the *Xenopus* Cx38 (Ebihara et al., 1989), mouse Cx37 (Willecke et al., 1991), or chicken Cx42 (Barrio et al., 1995) junctions. At the single-channel level, the existence of multiple conductance states of Cx43 and Cx32 channels with variable voltage sensitivity (Moreno et al., 1994; Valiunas et al., 1997; Oh et al., 1997) strictly precludes the application of a two-state Boltzmann equilibrium. In the present study, we have carried out the molecular dissection of the two kinetic components that characterize the V_j dependence of Cx32 and Cx43 conductance at the macroscopic level. We found that the truncation of the CT domain in both connexins eliminated the rapid component of g_j transitions. Furthermore, the results reveal that Cx32 and Cx43 conductance dependence involves the action of two separate V_j gates located in different molecular domains.

MATERIALS AND METHODS

Construction of CT truncated Cx32 and Cx43

Truncated human Cx32 at position 220 (HCx32-R220stop) and the rat Cx43 at position 257 (RCx43-S257stop) were obtained by the introduction of a premature stop codon into the wild-type cDNAs, using site-directed mutagenesis by inverse polymerase chain reaction with XLRTth polymerase (Perkin-Elmer, Langen, Germany). A cDNA of human Cx32 (kindly provided by N. M. Kumar) containing the complete coding region (Kumar and Gilula, 1986) was cloned into a pBlueScript vector containing 5′ and 3′ flanking regions of noncoding *Xenopus* β-globin sequence to boost expression (Gupta et al., 1994). To generate the HCx32-R220stop mutant, the following primers were used: sense 5′ TGATGCCACATCCAGGCAACCTG 3′ and antisense 5′ GCGGGCACAGGCCCGGATGATGAG 3′. The mutant RCx43-S257stop was obtained by amplification of the rat Cx43 cDNA (Beyer et al., 1987), inserted into the *Bgl*II site of the blunted *Eco*RI-*Hin*cII fragment of β-globin of a pSp64T plasmid, using the primers sense 5′ TGATATCACGACCTCCAGCAGAGC 3′, and antisense 5′ TGGGCTCAGTGGGCCAGTGGTGGC 3′. The polymerase chain reaction products were digested by *Dpn*I endonuclease to eliminate the template and with Pfu DNA polymerase to remove the bases extended onto the 3′ ends before ligation. Mutants were screened by size or restriction enzyme analysis and confirmed by DNA sequencing of the entire coding region on both strands.

Expression in paired *Xenopus* oocytes

Capped cRNAs of wild-type and HCx32-R220stop mutant were transcribed by T3 RNA polymerase from 10 μg of *Sal*I linearized plasmid, and the wild-type and truncated RCx43-S257stop by SP6 polymerase after a *Bam*HI digestion of plasmid. The cRNA synthesis and purification were performed as previously described (Barrio et al., 1997). Oocytes were removed from the ovaries of *Xenopus laevis* (Nasco, Fort Atkinson, WI) under anesthesia and prepared as described by Barrio et al. (1997). Oocytes (stage V and VI) were coinjected with an antisense oligonucleotide directed against *Xenopus* Cx38 mRNA, to block endogenous expression (10 ng/oocyte; Barrio et al., 1991), and with the in vitro transcribed cRNA of wild-type and mutants (0.1–0.5 μg/μl; 50 nl/oocyte). After 24 h, vitelline membranes were removed manually with forceps in hypertonic solution before oocytes were paired.

Measurement of junctional conductance

Pairs injected with cRNAs were recorded after 24–72 h in ND96 (in mM, 96 NaCl, 2 KCl, 1 $MgCl_2$, 1.8 $CaCl_2$, 5 HEPES, pH 7.45), using microelectrodes of 0.5–1 MΩ filled with 2 M KCl, 10 mM EGTA, and 10 mM HEPES (pH 7.20). The dual voltage clamp technique, in which each cell of the pair is impaled with two microelectrodes connected to an independent amplifier (TEV-200; Dagan, Minneapolis, MN), was used to measure the macroscopic junctional conductance (g_j). The procedure to measure g_j was as follows, where V_1, I_1, V_2, and I_2 are voltages and currents with the holding current subtracted in oocytes 1 and 2, respectively. First, the two oocytes were clamped at the same holding potential (V_h, e.g., −40 mV), whereby $V_j = 0$, because $V_j = V_1 - V_2$. To explore the influence of V_j on g_j, voltage steps of positive and negative polarities were applied in oocyte 1, defining a positive V_j as a greater relative positivity in oocyte 1. In this procedure the currents injected into oocyte 2 (I_2) to hold its potential constant were equal in magnitude and opposite in sign to the currents flowing through the junctional channels ($I_j = -I_2$), and the g_j was calculated as I_j/V_j. The stability of the junctional conductance was controlled by applying a small and brief prepulse just before each V_j step during the recording period. Stimulation and data collection were performed using a PC-AT computer, a Digidata 1200-A interface, and pCLAMP software (Axon, Foster City, CA), and junctional currents low pass filtered at 1 kHz. Full clamping voltage was reached 1–5 ms after the voltage onset. The time course of g_j transitions was fitted to exponential relations with $R < 0.999$, using Clampfit (pCLAMP).

Junctional conductance modeling

To evaluate the transjunctional voltage dependence of gap junctions, the macroscopic steady-state junctional conductance/voltage relationship was fit to a Boltzmann relation of the form (Spray et al., 1981) $G_{jss} = \{(G_{jmax} - G_{jmin})/(1 + \exp[A(V_j - V_0)])\} + G_{jmin}$, which applies to a two-state system, with the energy difference between states linearly dependent on voltage. Although not all channels may meet these assumptions (see Results), this analysis still provides useful parameters for comparing their behavior. The G_{jmax} is the maximum conductance, G_{jmin} is the residual conductance at large V_j or the voltage-insensitive component of the conductance, V_0 is the transjunctional voltage at which $G_{jss} = (G_{jmax} - G_{jmin})/2$, and A ($A = nq/kT$) is a constant that expresses the voltage sensitivity in terms of gating charge as the equivalent number (n) of electron charges (q) moving through the entire membrane voltage, and kT has its usual significance. Steady-state g_j values (g_{jss}) obtained by using pulses of sufficient duration were normalized relative to the g_j value for brief V_j prepulses (10 mV) and plotted versus voltage. The averaged G_{jss}/V_j relationships were well described by a single Boltzmann relation for each polarity of V_j, based on the assumption that each polarity of V_j affected a single gap junction hemichannel. Fits were made by treating G_{jmax}, G_{jmin}, A, and V_0 as free parameters, and the best values of constants were obtained by applying an iterative procedure of fitting to minimize the least-squares error between data and the calculated fit point (SigmaPlot; Jandel Scientific, Chicago, IL).

RESULTS

Two CT deleted connexins were examined in the present study, the human Cx32 truncated at position 220 and the rat Cx43 truncated at position 257. The HCx32-R220stop mutant has been identified in several families with the X-linked form of Charcot-Marie-Tooth disease (Fairweather et al.,

1994; Bone et al., 1995; Ionasescu et al., 1996), a hereditary peripheral neuropathy. The RCx43-S257stop mutant has been previously used by Delmar's group in studies of channel formation (Dunham et al., 1992), pH gating (Liu et al., 1993), and insulin-induced regulation (Homma et al., 1998). After 24 h of pairing, the electrical coupling between pairs of oocytes expressing CT-truncated and wild-type Cx43 did not differ significantly (Cx43: 14.67 ± 5.23 μS versus Cx43–257: 11.35 ± 4.82 μS; mean values ± SEM; $n = 27$ pairs from three experiments), whereas coupling was approximately twofold smaller in the case of truncated Cx32 relative to its corresponding wild-type pairs (Cx32: 12.33 ± 3.86 μS versus Cx32–220: 5.48 ± 2.27 μS; $n = 26$). This apparent decrease in the induction of coupling is consistent with previous studies, which have shown a striking correlation between the shortening of the carboxyl tail length and the level of coupling (Dunham et al., 1992; Rabadan-Diehl et al., 1994; Castro et al., 1999). It has previously been demonstrated that the lower coupling induced by truncated Cx32-R220stop is a result of the limited ability of hemichannels to assemble into complete gap junction channels (Castro et al., 1999). The decrease in the efficiency of forming complete channels was partially rescued by wild-type Cx32 hemichannels, because the heterotypic tailless wild-type pairs developed higher levels of coupling relative to the combinations of mutant alone (8.43 ± 3.63 μS; $n = 21$). These levels of coupling are intermediate between the homotypic tailless and wild-type junctions, indicating that the hemichannel-hemichannel assembly is a cooperative process, the efficiency of which results from the combined action of the two contributing hemichannels. To avoid differences between wild-type and mutated junctions attributable to the different levels of conductance and access resistance limitations (Wilders and Jongsma, 1992), only those pairs with similar levels of coupling and junctional conductance < 5 μS were included in the present study.

Deletion of the CT domain abolished the fast mechanism of V_j gating

The conductance of human Cx32 and rat Cx43 junctions is regulated by the transjunctional voltage or the voltage difference between the membrane potential of two cells. At the macroscopic level, the junctional conductance of both types of junctions decayed to lower values when V_j was increased from 0 to +100 mV and increased again to high values when V_j was reduced from +100 to +20 mV, a voltage too small to affect coupling (Fig. 1 *A*). The time course for the decay of junctional currents and their recovery had two components with fast and slow time constants. The Cx32 and Cx43 transitions diverged in the fractional amplitude of the two components, because the rapid process was dominant in the case of the Cx43 g_j, whereas the slow process was the major component of the Cx32 conductance changes. These data are consistent with previous kinetic analyses of the relaxation of junctional currents between cells connected by Cx43 channels (Moreno et al., 1992; Wang et al., 1992; Lal and Arnsdorf, 1992) and by Cx32 channels (Verselis et al., 1994). Interestingly, the application of the V_j protocol between pairs coupled by junctions composed of CT truncated Cx32 or Cx43 induced changes of g_j with a unique component of decay and recovery that followed a slow time course (Fig. 1 *B*). Thus the truncation of the CT tail in both types of junction abolished the rapid component of their g_j transitions, revealing the existence of two separate V_j gatings underlying each of the two kinetic processes, where the CT domain is likely to be an integral part of the fast gate.

V_j gating properties of the tailless Cx32 and Cx43 junctions

The V_j dependence of the truncated Cx32 and Cx43 junctions was studied in detail (Figs. 2 and 3). Differences between the wild-type and truncated junctions were quantified in terms of their kinetic properties and of the steady-state G_j/V_j relationships. The junctional conductance of wild-type HCx32 channels was at maximum at zero V_j and decreased symmetrically in response to positive and negative $V_j \geq +20$ mV, with progressively larger and faster reductions at larger V_j's. The g_j reductions showed a characteristic biphasic time course with an initial closing of small amplitude and fast kinetics observable with high-resolution records, and a second component with a slower time course, which mediated the major part of the g_j response to the long-lasting pulses (Fig. 2 *A*, *top*). The conductance of the truncated HCx32-R220stop junctions also decreased with larger and faster reductions for increasing V_j's; however, the time course of the current decay had a unique kinetic component because the fast component was not present (Fig. 2 *A, bottom*). Thus the g_j decays of the wild-type and tailless junctions were well fitted by biexponential and monoexponential functions, respectively (Fig. 2 *B*, *insets*). The time constants of high to low conductance transitions were roughly symmetrical for positive and negative pulses and briefer for increasing V_j's (Fig. 2 *B*). Representative examples of the time constants for V_j pulses of −100 mV were $\tau_1 = 109 \pm 24$ ms and $\tau_2 = 4.75 \pm 0.55$ s, with a ratio of amplitudes between major and minor components of 5. For the same V_j pulse, the mean value of the time constant for the unique component of the truncated junctions was $\tau = 1.83 \pm 0.58$ s, which is approximately threefold briefer than the corresponding value of the slow component in the wild-type junction. There were also differences between wild-type and truncated steady-state G_j/V_j relationships (Fig. 2 *C*). The curve of the truncated junctions was shifted toward smaller V_j's and had lower values of residual conductance. The G_j/V_j relationship for each V_j polarity was well described by a single Boltzmann relation, whose parameters of fitting showed little if any difference in voltage sensitivity, A, a reduction of half-voltage activation, V_0, of ~10 mV, and a decrease in the residual conductance, G_{jmin}, of 5–10% (Table 1).

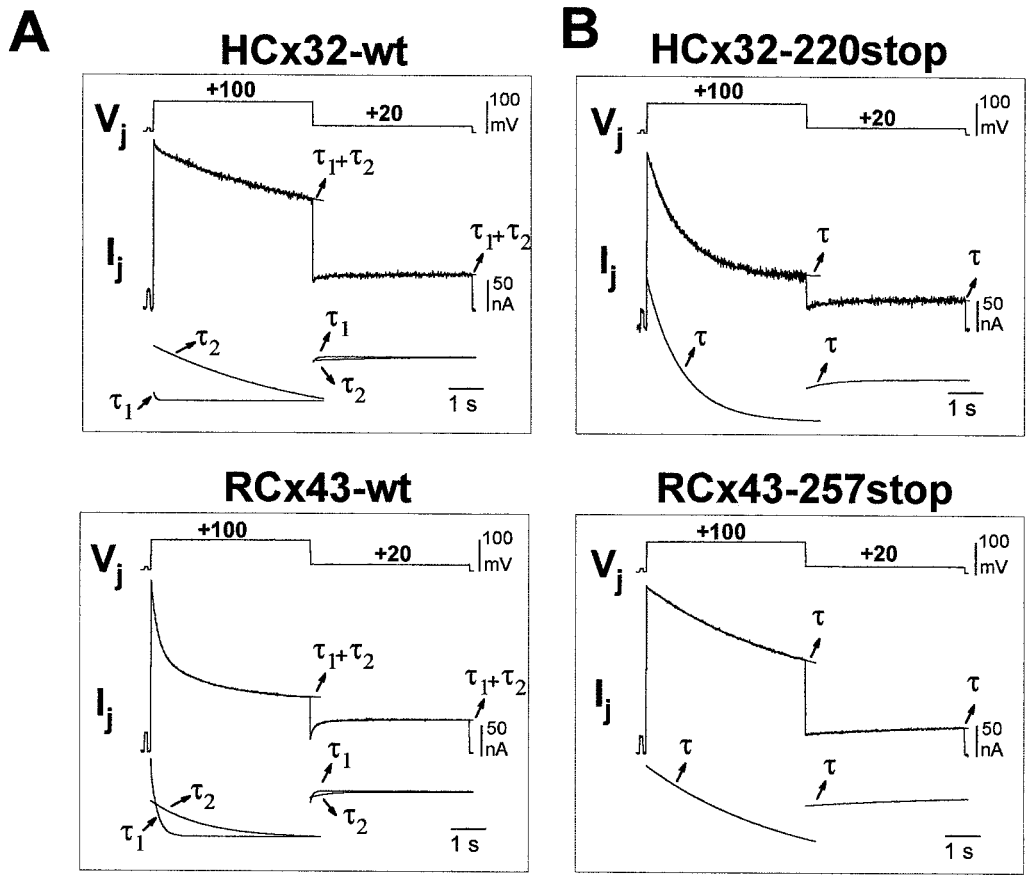

FIGURE 1 Truncation of the carboxyl terminal domain abolished the fast V_j-sensitive component of the Cx32 and Cx43 junctional conductance. Changes in wild-type and CT truncated human Cx32–220stop and rat Cx43–257stop junctional currents (I_j) were induced by transjunctional voltage (V_j) steps of 5 s duration varying from 0 to +100 mV and returning to +20 mV. (*A*) The time courses of the macroscopic I_j's decay and recovery of both wild-type junctions (HCx32-wt; RCx43-wt) were fitted to biexponential relations (τ_1 and τ_2). The rapid component is the minor component in the Cx32 junctions, whereas this is the dominant component in the case of Cx43 conductance. (*B*) Conductance transitions of the Cx32 and Cx43 tailless junctions required a monoexponential fitting with slow time constants (τ). Data revealed the existence of two separate gatings located in different domains of the connexin molecule.

The deletion of the CT tail of RCx43 induced qualitatively similar novel V_j gating properties. The wild-type and truncated Cx43 junctions responded to the application of positive and negative V_j steps of increasing magnitude (±100 mV) with progressively larger and faster g_j reductions (Fig. 3 *A*, *top* and *bottom*). However, while the wild-type current decay followed a biexponential time course, the transitions of truncated junctions were monoexponential, with slow time constants of several seconds (Fig. 3 *B*, *insets*). Time constants of wild-type junctions became shorter at larger V_j's and were slightly briefer at negative rather than positive V_j polarity. At the V_j pulse of −100 mV, illustrative examples were a $\tau_1 = 417 \pm 175$ ms and $\tau_2 = 7.06 \pm 1.28$ s, with a ratio of amplitudes between the fast and slow components of 3. In the case of the tailless junctions, the currents decayed in a monoexponential fashion with briefer time constants than those of the slow component in the wild-type junctions (Fig. 3 *B*). Differences between wild-type and truncated Cx43 channels were also quantified in terms of the steady-state G_j/V_j relationships. The asymmetry of the G_j/V_j curve for positive and negative V_j's that distinguishes the wild-type Cx43 junctions (Banach and Weingart, 1996) disappeared upon CT truncation, and the Boltzmann parameters showed a marked reduction (10–20%) of the characteristic large residual conductance of Cx43 junctions as well as minor differences in voltage sensitivity (Table 1).

In summary, the deletion of the CT domain in the two different connexin isoforms, Cx43 and Cx32, had similar effects on their V_j dependencies. Both types of tailless junctions lost the fast V_j gating, and in the absence of this fast mechanism, the voltage-sensitive component of junctional conductance increased.

Fast and slow processes of gating are intrinsic properties of hemichannels

When oocytes expressing the wild-type and tailless connexins were paired, coupling developed between them. The V_j

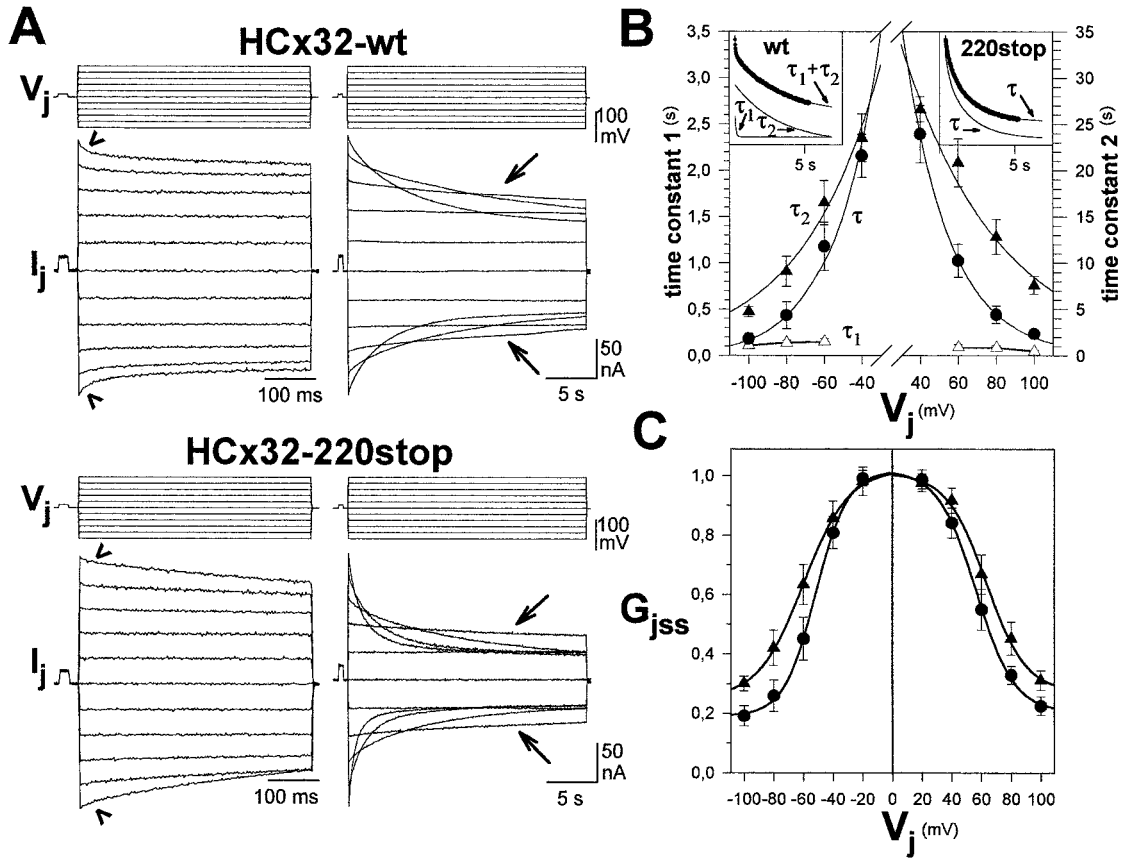

FIGURE 2 Comparison of the V_j gating properties between wild-type and tailless HCx32 junctions. (*A*) Sample records of junctional currents (I_j) of wild-type (*top*) and truncated (*bottom*) junctions evoked by V_j pulses of ±100 mV in 20-mV increments, of 500 ms and 30 s duration (*left and right*). Deletion of Cx32 CT abolished the rapid component (*left, arrowheads*) and induced faster and larger I_j decays (*right, arrows*). (*B*) V_j dependence of the time constants. The time course of wild-type currents required biexponential fits, whereas the tailless junctions followed monoexponential relations (*insets*). Time constants (τ_1 and τ_2) decreased symmetrically for larger positive and negative V_j's; the slow τ of deleted junctions was briefer than the wild-type τ_2. (*C*) Graph of the steady-state G_j/V_j relationships. The curve of truncated junctions (*circles*) was shifted toward smaller voltages and had a smaller residual conductance relative to wild type (*triangles*). The G_{jss}/V_j relationships were well fitted to a Boltzmann function for each V_j polarity with the parameters of Table 1. Each point in *B* and *C* represents the mean value (± SEM) of six pairs.

effects on g_j of the hybrid HCx32wt/HCx32-R220stop and RCx43wt/RCx43-S257stop junctions are illustrated in Fig. 4. In agreement with the heterotypic hemichannel composition of the junctions, currents in response to positive and negative V_j pulses were asymmetrical (Fig. 4 *A*). V_j pulses negative in the oocyte expressing the wild-type hemichannels induced junctional currents that resembled those elicited by V_j in the respective homotypic wild-type HCx32 or RCx43 junctions, shown in Figs. 2 and 3, respectively. Responses to positive V_j, which are seen as relative negativities from the cytoplasmic side of the truncated hemichannels, were also similar to those of the homotypic truncated, HCx32-R220stop and RCx43-S257stop, junctions (Figs. 2 and 3). Accordingly, the time courses of current decay in response to negative V_j's in the side of the wild-type hemichannels required a biexponential fit for both types of hybrid junctions, whereas for negative V_j's, truncated hemichannels were well fitted by a monoexponential function (Fig. 4 *B*, *insets*), as was previously described for the respective parent junctions.

The relation between the time constant and the steady-state G_j versus voltage of the hybrid channels was plotted with the curves of the respective homomeric junctions. The two curves overlapped almost perfectly in the case of the RCx43wt/RCx43–257stop channels and with minor deviations for the HCx32wt/HCx32-R220stop junctions (Fig. 4, *B* and *C*). The voltage dependence of the time constants in the HCx32-R220stop side was shifted toward a somewhat smaller voltage, and these changes in kinetics were consistent with a small shift in the G_j/V_j relationship to less negative V_j values. In the HCx32 hemichannel side, the amplitude of the fast component increased somewhat and its kinetics accelerated slightly, while time constants of the slow gating changed in the opposite way. In summary, the data indicate that 1) the characteristics of V_j gating processes are little affected by the association of wild-type hemichannels with the truncated hemichannels; 2) there are independent V_j gates in each hemichannel: one fast and one slow gate in the wild-type HCx32 or RCx43 hemichannels, whereas only the slow gate is present in the CT truncated

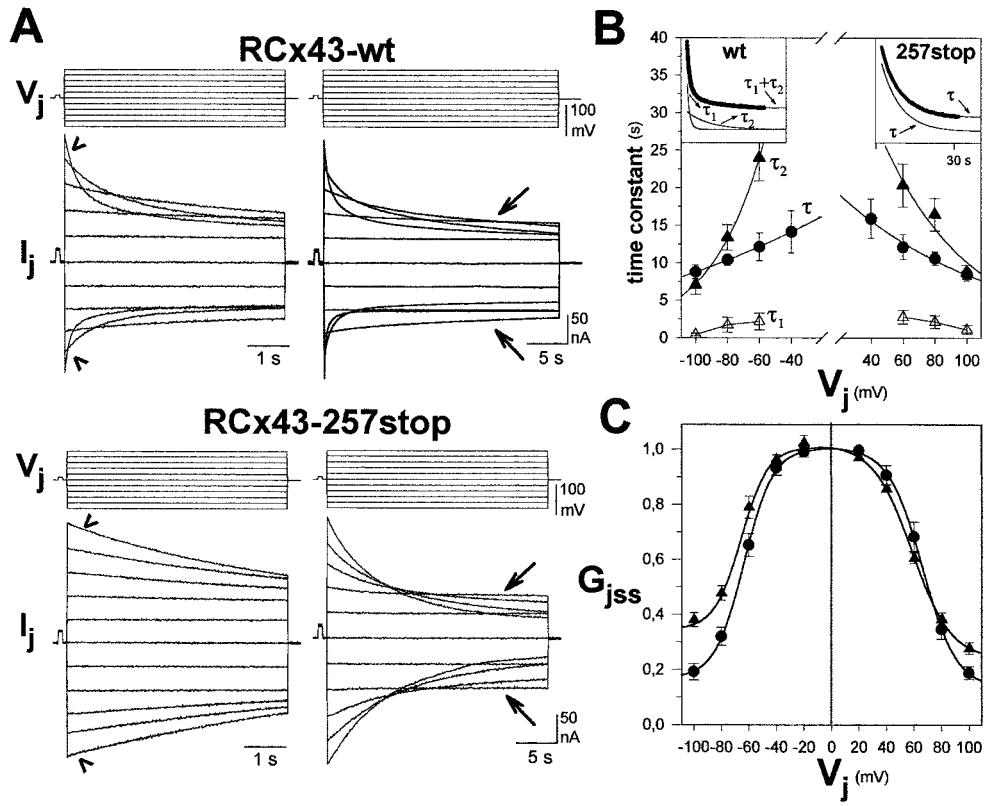

FIGURE 3 Comparison of the V_j gating properties of wild-type and tailless RCx43 junctions. (*A*) Sample records of junctional currents (I_j) of wild-type (*top*) and truncated (*bottom*) junctions evoked by the same V_j protocols as in Fig. 2. The CT truncation of Cx43 eliminated the fast component (*left, arrowheads*) and induced larger I_j reductions (*right, arrows*). (*B*) V_j dependence of the time constants. The wild-type currents followed biexponential time courses, whereas the tailless current decay was monoexponential (*insets*). Time constants (τ_1 and τ_2) of wild-type junctions decreased asymmetrically for larger V_j 's of both polarities, whereas the changes in the unique time constant of the deleted junctions were symmetrical and briefer than wild-type τ_2. (*C*) Graph of the steady-state G_j/V_j relationships. Wild-type G_{jss}/V_j relations (*triangles*) were asymmetrical, with lower conductances for positive than for negative voltages, whereas the curve of the tailless junctions (*circles*) was symmetrical and had lower values of residual conductance. Curves were well fitted to a Boltzmann function for each V_j polarity with the parameters of Table 1. Each point in *B* and *C* represents mean values (± SEM) of six pairs.

HCx32 or RCx43 hemichannels; and 3) the two gates seem to close at negative V_j on the cytoplasmic side. A negative polarity of closure was previously identified for the slow Cx32 V_j gating by point mutation analyses (Verselis et al., 1994) and inferred for Cx43 hemichannels from various heterotypic combinations (Moreno et al., 1995; Banach et al., 1998; Martin et al., 1998).

DISCUSSION

Two mechanisms of gating mediate the V_j dependence of Cx32 and Cx43 junctions

The main conclusion arising from the present work is that the V_j-dependent conductance of rat Cx43 and human Cx32

TABLE 1 Boltzmann parameters of V_j dependence for wild-type and CT truncated Cx32 and Cx43 junctions

	V_j (−)					V_j (+)				
	A	n	V_0	G_{jmax}	G_{jmin}	A	n	V_0	G_{jmax}	G_{jmin}
HCx32-HCx32	0.07	1.77	60.0	1.02	0.25	0.07	1.77	63.2	1.01	0.27
220stop-220stop	0.09	2.27	51.8	1.02	0.19	0.08	2.02	56.4	1.02	0.20
HCx32-220stop	0.13	3.28	58.2	1.01	0.27	0.11	2.78	47.8	1.03	0.19
RCx43-RCx43	0.10	2.56	65.7	1.02	0.36	0.07	1.77	58.5	1.02	0.24
257stop-257stop	0.09	2.27	63.5	1.00	0.16	0.08	2.02	66.2	1.01	0.13
RCx43-257stop	0.09	2.27	62.9	1.02	0.37	0.07	1.77	60.7	1.01	0.19

Junctional conductance for each V_j polarity was described by a single Boltzmann relation, based on the assumption that each polarity of V_j affected a single gap junction hemichannel. A, voltage sensitivity (mV^{-1}); n, calculated gating charge at 20°C; V_0, voltage value of half-inactivation in g_j (mV); G_{jmax}, theoretical maximum conductance extrapolated from the experimental data; G_{jmin}, extrapolated values of residual conductance. In the case of the hybrid, negative V_j are defined as relative negativity in the cytoplasmic side of the cell expressing the wild-type hemichannels.

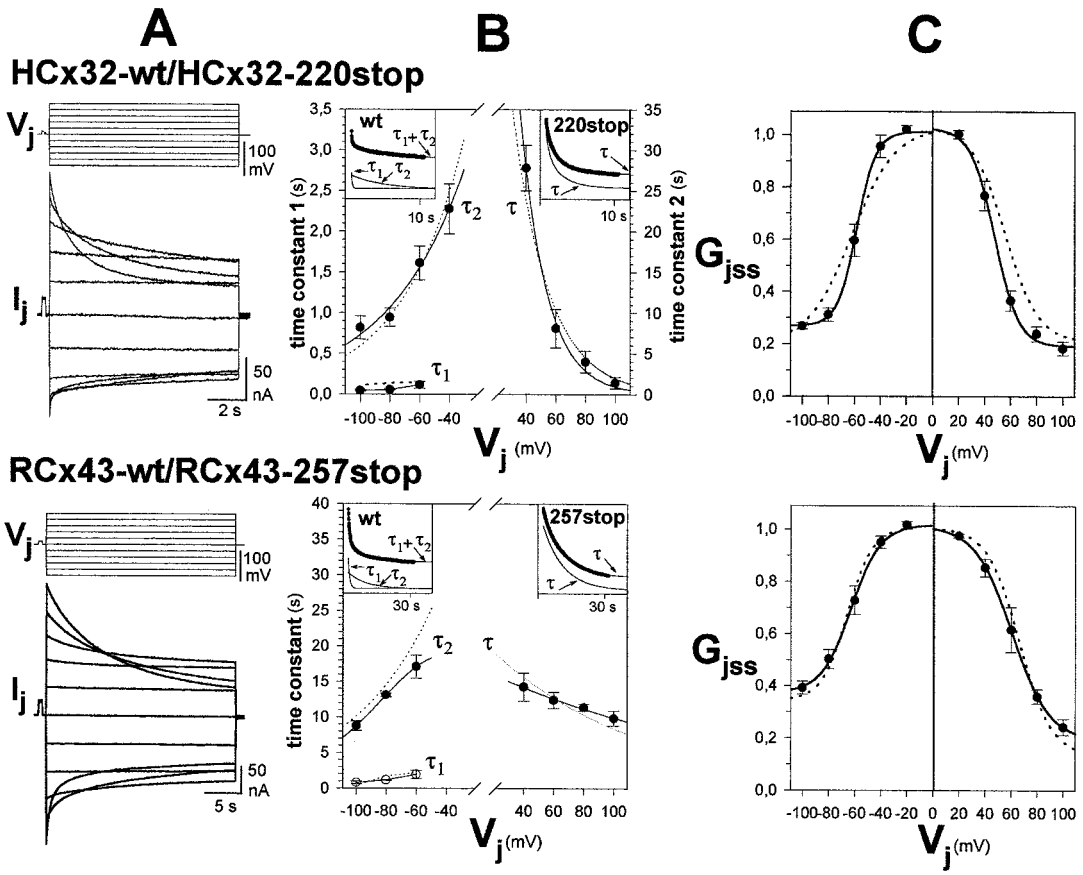

FIGURE 4 V_j gating properties of the hybrid wild-type/tailless junctions. (*A*) Sample records of junctional currents (I_j) induced by V_j pulses in 20-mV increments up to ±100 mV, of 10 s duration for hybrid HCx32-wt/HCx32–220stop junctions (*top*) and 30 s duration for RCx43-wt/RCx43–257stop junctions (*bottom*). Positive and negative V_j polarities are defined as relative depolarization and hyperpolarization of the cell expressing the wild-type hemichannels, which induced upward and downward I_j's, respectively. (*B*) V_j dependence of the time constants. Junctional currents in response to negative pulses followed biexponential time courses, whereas at positive V_j, which are seen as negativities from the tailless hemichannel side, were monoexponential (*insets*). Time constants of wild-type (τ_1 and τ_2) and of truncated hemichannels (τ) were plotted with those of the corresponding homomeric junctions (*dotted curve*). (*C*) Graph of the steady-state G_j/V_j relationships. Mean G_{jss} values of the hybrid junctions were well fitted to a Boltzmann function for each polarity (——) with the parameters of Table 1 and plotted with their parent homotypic junctions (·····). Gating properties attributable to wild-type and truncated hemichannels for negative V_j's were largely conserved in the corresponding heterotypic junctions. Each point in *B* and *C* represents a mean value (± SEM) of six pairs.

junctions involves the combined action of two separable gates. The wild-type RCx43 and HCx32 junctions responded to V_j with a fast and slow kinetic component, whereas those composed of the truncated CT connexins was exclusively regulated by a slow V_j gating process. Thus the two kinetic components of the Cx43 and Cx32 junctions may represent two different mechanisms of gating, the CT domain being wholly responsible for the fast V_j gating. The remote possibility that tailless junctions actually lose the slow component and slow down the fast one cannot be entirely excluded, but this alternative interpretation seems less probable because the kinetic properties of truncated junctions are closer to those of the slow component in the wild-type junctions. Additional experimentation will be required to test whether the V_j dependence of other junctions is also mediated by two gating processes, especially in those junctions in which conductance clearly exhibits a double range of V_j sensitivities, such as the *Xenopus* Cx38 (Ebihara et al., 1989), mouse Cx37 (Willecke et al., 1991), or chicken Cx42 junctions (Barrio et al., 1995).

Information about the three-dimensional structure of gap junction channels shows two connexons or hemichannels, each with six connexin molecules and an open pore in the connexon center (Makowski et al., 1977, Unwin and Zampighi, 1980; Hoh et al., 1991; Unger et al., 1997). Two different gating mechanisms have been proposed, the constriction of the channel pore by tilting and twisting of the six subunits (Unwin and Ennis, 1984), and the closing of the mouth of the pore by a six-segmented barrier at the cytoplasmic surface (Makowski et al., 1984). The general topology of connexins has already been confirmed in the case of Cx32 and Cx43 by proteolysis and antibody binding experiments (Zimmer et al., 1987; Hertzberg et al., 1988; Milks et al., 1988; Goodenough et al., 1988; Yancy et al., 1989; Yeager and Gilula, 1992). The abolition of the fast V_j gating mechanism by deletion of the CT suggests that this

gate may operate in a way similar to that of the "ball-and-chain" model of gating that mediates the fast inactivation in other unrelated families of ionic channels (reviewed by Amstrong and Hille, 1998). However, there are at least two main differences between this type of gating and the ball-and-chain inactivation hypothesis initially proposed for the ShakerB potassium channels (Hoshi et al., 1990). First, the K^+ channels open and then quickly inactivate during a depolarization, whereas gap junction channels can remain open in the absence of a V_j gradient without any spontaneous inactivation. Thus we prefer to consider the closing process of gap junction channels as deactivation rather than inactivation. Second, the N-inactivation rate is voltage independent, whereas the fast V_j gating is subject to the electric field and channels close in response to V_j's of negative polarity, as seen on the cytoplasmic side. The fast gating reaction may consist of the displacement of the CT, a structure rich in charged residues, toward the inner mouth of the channel, which behaves like a partial open-channel blocker. Several lines of evidence imply that the CT of connexins is a movable structure. Based on structural analysis of the cytoplasmic surface, it has been proposed that the structure at the carboxyl tail be disordered, apparently because of peptide flexibility in this region (reviewed by Sosinsky, 1992, 1996). In this context, it is also interesting to note that the V_j gating properties of the tailless RCx43 junctions reported here are identical to those of the junctions composed of chimeric Cx43-aequorin proteins (see figure 4 in Martin et al., 1998). In those experiments, aequorin, a calcium indicator of high molecular mass (22 kDa), was fused in frame to the CT of a full-length RCx43. In accordance with a "ball-and-chain" model, the loss of the fast mechanism of gating might be caused by the limited mobility of the CT domain fused to a large molecule. An alternative explanation may be that the aequorin fusion would alter the conformational determinants required as a "particle" in a "particle-receptor" model of gating.

It has previously been demonstrated that the CT tail of Cx43 plays an important role in pH gating. The RCx43–257stop junctions lose their higher sensitivity pH gating (Liu et al., 1993), and pH sensitivity was partly restored when the portion of the CT deleted was expressed separately from the rest of the protein (Morley et al., 1996). Based on these data, a "particle-receptor" model has been proposed for Cx43 pH gating. Upon intracellular acidification, the CT would bind noncovalently to a separate specific domain, acting like a receptor site in the mouth of the pore. Protonation of histidine residues located at the cytoplasmic loop may be part of the receptor (Ek et al., 1994). More recent results suggest that the "particle-receptor" model is also applicable to other types of chemical regulation, such as the closure of Cx43 junctions induced by insulin or insulin-like growth factor-1 (Homma et al., 1998) and $pp60^{v\text{-}src}$ oncogene (Nicholson et al., 1998). Thus it seems that these are independent modes of coupling regulation by voltage or chemical agents, such as pH and phosphorylation. They may share a common gating mechanism, although the structure-function determinants may not be the same, and they have a different time course. Further investigation is needed to determine the regions of the CT that are necessary for the fast V_j gating, and of the inner pore-forming region that would be its specific receptor.

A wide body of evidence suggests that the slow V_j gating mechanism involves a "global" conformational change of the channel. The V_j sensor has been associated with the charged residues in the NT and the border of first transmembrane domain and the first extracellular loop of rat Cx32 and Cx26 (Verselis et al., 1994). Based on the dramatic effects of the substitution of a conserved proline in M2, which even induced reversion of the polarity of channel closure, it has been proposed that this proline plays a central role in the transduction of the signal leading to channel closure (Suckyna et al., 1993). Moreover, the voltage properties associated with slow gating can be modified to a variable degree by the docking interactions between hemichannels, an effect that depends critically on the type of connexin in the apposed hemichannel (e.g., see Fig. 4; Hennemann et al., 1992; Barrio et al., 1997). Taken together, the data indicate that the properties of the slow gating derive from the complex interactions among various portions of the molecule, and that specificity does not reside exclusively at the level of primary sequence.

A novel V_j gating model of Cx43 and Cx32 junctions

The existence of two separable mechanisms of gating controlled by V_j leads to a novel model underlying the transjunctional voltage dependence of gap junction channels. Because the two gating elements are believed to reside in different connexin domains, one would expect no change of slow V_j gating properties between wild-type and tailless channels. However, the deletion of the CT domain in both connexin isoforms, Cx32 and Cx43, produced, in addition to the loss of the fast mechanism of gating, an increase in the V_j-sensitive component of the junctional conductance. Such changes in properties attributable to the slow gating mechanism may indicate that the fast and slow gates do not operate independently. Several possible types of interactions could take place between the two gates, depending on where they are located with respect to each other and the channel's bore geometry. Assuming that the fast gate is located in the cytoplasmic CT domain farther away from the channel bore than the slow gate, a simple interpretation of the novel properties of slow gating is that the two mechanisms of gating interact electrically in series (Fig. 5). The sequence of reactions would be as follows. First, a negative V_j would induce the closure of the rapid gate, which might be caused by the displacement of the CT domain toward the inner mouth of the channel, producing the partial occlusion of the pore. Then the closure of the slow gate would follow, which might involve a global conformational change of the channel, and induce an additional decrease in conductance.

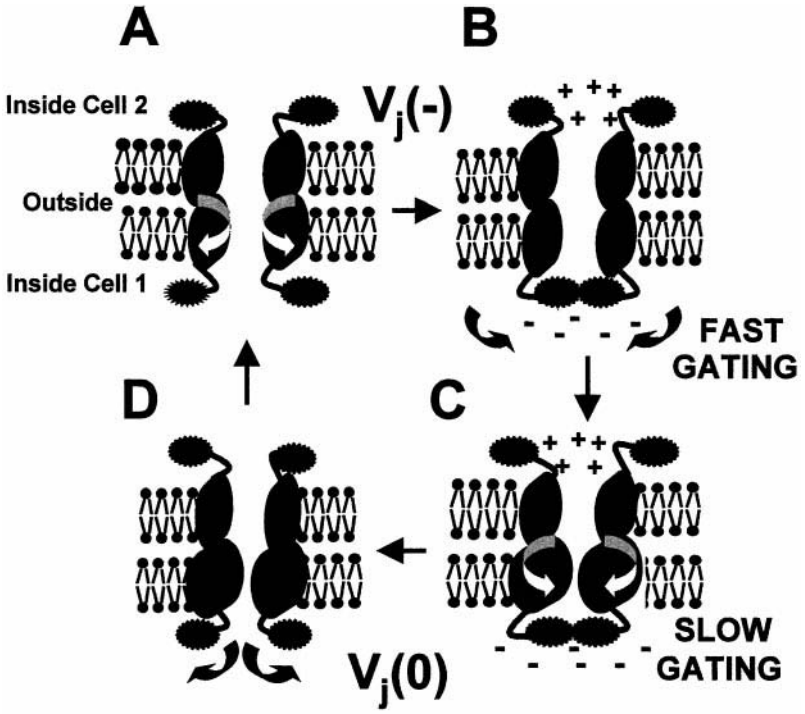

FIGURE 5 V_j gating model of the RCx43 and HCx32 junctions. The novel model proposed contains two mechanisms of V_j gating, one fast gate and one slow gate in each hemichannel, interacting electrically in series. (*A*) When $V_j = 0$, both gates are open. (*B*) In response to a negative V_j gradient, defined as relative negativity in the cytoplasmic side, the CT domain, proposed to be an integral part of the rapid gate, might displace toward the inner mouth of the channel and cause a partial physical occlusion of the pore. (*C*) Then an additional decrease in conductance may occur because of the closure of the slow gate as a result of a global conformational motion of the channel structure. (*D*) Returning V_j to zero, the CT gate opens first, and the slow gating later leads to a fully open channel (in *A*). According to the assumption that the sensor associated with the slow gating is sensing the V_j throughout the pore, the closure of the fast gate would cause an increase in the voltage drop, reducing the V_j seen by the sensor of the slow gating.

As V_j returns to zero, the fast gate opens first and then the slow gate. According to the current assumption that the voltage sensor associated with the slow gating responds to the V_j throughout the pore lumen (Harris et al., 1981), a partial occlusion of the channel mouth would increase access resistance and so cause a larger voltage drop. Consequently, the sensor might be seeing smaller V_j's when the fast gate is present than when it is abolished. If this is so, larger and faster conductance reductions would be expected at smaller voltages, as occurred experimentally in the case of truncated Cx43 and Cx32 junctions. At present, the possibility that the CT truncation by itself may induce a conformational change that alters the properties of the slow gating cannot be completely ruled out. In this context, the larger changes in slow gating than expected in the case of Cx32–220stop junctions may be an indication that the most proximal region of CT domain is also an important determinant of the slow V_j gating properties.

At the single-channel level, the reduction of conductance after large V_j pulses has been associated with transitions between the fully open state or substates to a residual open substate, and, less frequently, with the fully closed state (Moreno et al., 1994; Valiunas et al., 1997; Oh et al., 1997). Thus the existence of a residual open state of low conductance has been proposed as an explanation for the incomplete macroscopic g_j closing, G_{jmin}, observed even at larger V_j's. Now a more detail analysis is required to identify the transitions between different conductance states specifically mediated by the fast and slow V_j gatings.

REFERENCES

Amstrong, C., and B. Hille. 1998. Voltage-gated ion channels and electrical excitability. *Neuron.* 20:371–380.

Banach, K., S. V. Ramanan, and P. R. Brink. 1998. Homotypic hCx37 and rCx43 and their heterotypic form. *In* Gap Junctions. R. Werner, editor. IOS Press, Amsterdam. 76–80.

Banach, K., and R. Weingart. 1996. Connexin43 gap junctions exhibit asymmetrical gating properties. *Pflüger Arch Eur. J. Physiol.* 432: 775–785.

Barrio, L. C., J. Capel, J. A. Jarillo, C. Castro, and A. Revilla. 1997. Species-specific voltage-gating properties of connexin-45 junctions expressed in *Xenopus* oocytes. *Biophys. J.* 73:757–769.

Barrio, L. C., J. A. Jarillo, J. C. Sáez, and E. C. Beyer. 1995. Comparison of voltage dependence of chick connexin 45 and 42 channels expressed in pairs of *Xenopus* oocytes. *In* Progress in Cell Research: Gap Junctions, Vol. 4. Y. Kanno, K. Kataoka, Y. Shiba, Y. Shibata, and T. Shimazu, editors. Elvesier, Amsterdam. 391–394.

Barrio, L. C., A. Revilla, J. M. Gómez-Hernadez, M. DeMiguel, and D. Gonzalez. 1999. Membrane potential dependence of gap junctions in vertebrates. *In* Current Topics in Membranes: Gap Junctions—Molecular Basis of Cell Communication in Health and Disease. C. Pericchia, editor. Academic Press, San Diego. (in press)

Barrio, L. C., T. Suchyna, T. Bargiello, L. X. Xu, R. S. Roginski, M. V. L. Bennett, and B. J. Nicholson. 1991. Gap junctions formed by connexins 26 and 32 alone and in combination are differently affected by applied voltage. *Proc. Natl. Acad. Sci. USA.* 88:8410–8414.

Bennett, M. V. L., L. C. Barrio, T. A. Bargiello, D. C. Spray, E. Hertzberg, and J. C. Sáez. 1991. Gap junctions: new tools, new answers, new questions. *Neuron.* 6:305–320.

Bennett, M. V. L., and V. K. Verselis. 1992. Biophysics of gap junctions. *Semin. Cell Biol.* 3:29–47.

Beyer, E. C., D. L. Paul, and D. A. Goodenough. 1987. Connexin 43: a protein from rat heart homologous to a gap junction protein from liver. *J. Cell Biol.* 105:2621–2629.

Bone, L. J., N. Dahl, M. W. Lensch, P. F. Chance, T. Kelly, E. Le Guern, S. Magi, G. Parry, H. Shapiro, S. Wang, and K. H. Fischbeck. 1995. New connexin32 mutations associated with X-linked dominant Charcot-Marie-Tooth disease. *Neurology.* 45:1863–1866.

Bruzzone, R., J.-A. Haefliger, R. L. Gimlich, and D. L. Paul. 1993. Connexin40, a component of gap junctions in vascular endothelium, is restricted in its ability to interact with other connexins. *Mol. Biol. Cell.* 4:7–20.

Bruzzone, R., T. W. White, and D. L. Paul. 1996. Connections with connexins: the molecular basis of direct intercellular signaling. *Eur. J. Biochem.* 238:1–27.

Castro, C., J. M. Gómez-Hernandez, K. Silander, and L. C. Barrio. 1999. Altered formation of hemichannels and gap junction channels caused by C-terminal connexin-32 mutations. *J. Neurosci.* 19:3752–3760.

Dunham, B., S. Liu, S. Taffet, E. Trabda-Janik, M. Delmar, R. Tetryshyn, S. Zheng, R. Perzova, and M. L. Vallano. 1992. Immunolocalization and expression of functional and nonfunctional cell-to-cell channels from wild-type and mutant rat heart connexin43 cDNA. *Circ. Res.* 70: 1233–1243.

Ebihara, L., E. C. Beyer, K. I. Swenson, D. L. Paul, and D. A. Goodenough. 1989. Cloning and expression of a *Xenopus* embryonic gap junction. *Science.* 243:1194–1195.

Ek, J. F., M. Delmar, R. Perzova, and S. M. Taffet. 1994. Role of histidine 95 on pH gating of the cardiac gap junction protein connexin43. *Circ. Res.* 74:1058–1064.

Fairweather, N., C. Bell, S. Cochrane, J. Chelly, S. Wang, M. L. Mostacciuolo, A. P. Monaco, and N. E. Haites. 1994. Mutations in the connexin 32 gene in X-linked dominant Charcot-Marie-Tooth disease (CMTX1). *Hum. Mol. Genet.* 3:29–34.

Goodenough, D. A., D. L. Paul, and L. Jesaitis. 1988. Topological distribution of two connexin32 antigenic sites in intact and split rodent hepatocyte gap junctions. *J. Cell Biol.* 107:1817–1824.

Gupta, V. K., V. M. Berthoud, N. Atal, J. A. Jarillo, L. C. Barrio, and E. C. Beyer. 1994. Bovine connexin44, a lens gap junction protein: molecular cloning, immunological characterization and functional expression. *Invest. Ophthalmol. Vis. Sci.* 35:3747–3758.

Harris, A., D. C. Spray, and M. V. L. Bennett. 1981. Kinetic properties of a voltage-dependent junctional conductance. *J. Gen. Physiol.* 77:95–117.

Hennemann, H., T. Suckyna, H. Lichtenberg-Fraté, S. Jungbluth, E. Dahl, J. Swarz, B. J. Nicholson, and K. Willecke. 1992. Molecular cloning and functional expression of mouse connexin40, a second gap junction gene preferentially expressed in lung. *J. Cell Biol.* 117:1299–1310.

Hertzberg, E. L., R. M. Disher, A. A. Tiller, Y. Zhou, and R. G. Cook. 1988. Topology of the M_r 27,000 liver gap junction protein cytoplasmic localization of the amino and carboxyl termini and a hydrophobic domain which is protease hypersensitive. *J. Biol. Chem.* 265:2138–2147.

Homma, N., J. L. Alvarado, W. Coombs, K. Stergiopoulos, S. M. Taffet, A. F. Lau, and M. Delmar. 1998. A particle-receptor model for insulin-induced closure of connexin43 channels. *Circ. Res* 83:27–32.

Hoshi, T., W. N. Zagotta, and R. W. Aldrich. 1990. Biophysical and molecular mechanisms of Shaker potassium channel inactivation. *Science.* 250:533–538.

Ionasescu, V. V., R. Ionasescu, and C. Searb. 1996. Correlation between connexin 32 gene mutations and clinical phenotype in X-linked dominant Charcot-Marie-Tooth neuropathy. *Am. J. Med. Genet.* 63:486–491.

Kumar, N. M., and N. B. Gilula. 1986. Cloning and characterization of human and rat liver cDNAs coding for a gap junction protein. *J. Cell Biol.* 103:767–776.

Lal, R., and M. F. Arnsdorf. 1992. Voltage dependent gating and single-channel conductance of adult mammalian atrial gap junctions. *Circ. Res.* 71:737–743.

Liu, S., S. Taffet, L. Stoner, M. Delmar, M. L. Vallano, and J. Jalife. 1993. A structural basis for the unequal sensitivity of the major cardiac and liver gap junctions to intracellular acidification: the carboxyl tail length. *Biophys. J.* 64:1422–1433.

Makowski, L., D. L. Caspar, W. C. Phillips, and D. A. Goodenough. 1977. Gap junction structures. Analysis of the x-ray diffraction data. *J. Cell Biol.* 74:629–645.

Makowski, L., D. L. Caspar, W. C. Phillips, and D. A. Goodenough. 1984. Gap junction structures. V. Structural chemistry inferred from x-ray diffraction measurements on sucrose accessibility and trypsin susceptibility. *J. Mol. Biol.* 174:449–481.

Martin, P. E. M., C. H. George, C. Castro, J. M. Kendall, J. Capel, A. K. Campbell, A. Revilla, L. C. Barrio, and W. H. Evans. 1998. Assembly of chimeric connexin-aequorin proteins into functional gap junction channels. *J. Biol. Chem.* 273:1719–1726.

Milks, L. C., N. M. Kumar, R. Houghton, N. Unwin, and N. B. Gilula. 1988. Topology of the 32-kd liver gap junction determined by site-directed antibody localizations. *EMBO J.* 7:2967–2975.

Moreno, A. P., G. I. Fishman, E. C. Beyer, and D. C. Spray. 1995. Voltage dependent gating and single channels analysis of heterotypic gap junctions formed of Cx45 and Cx43. *In* Progress in Cell Research: Intracellular Communication Through Gap Junctions, Vol 4. Y. Kanno, K. Kataoka, Y. Shiba, Y. Shibata, and T. Shimazu, editors. Elvesier, Amsterdam. 405–408.

Moreno, A. P., G. I. Fishman, and D. C. Spray. 1992. Phosphorylation shifts unitary conductance and modifies voltage dependent kinetics of human connexin43 gap junction channels. *Biophys. J.* 62:51–53.

Moreno, A. P., M. B. Rook, G. I. Fishman, and D. C. Spray. 1994. Gap junction channels: distinct voltage-sensitive and insensitive conductance states. *Biophys. J.* 67:113–119.

Morley, G. E., S. M. Taffet, and M. Delmar. 1996. Intramolecular interactions mediate the pH regulation of connexin43. *Biophys. J.* 70: 1294–1302.

Nicholson, B. J., T. Suchyna, L. X. Xu, P. Hammernick, F. L. Cao, C. Fourtner, L. C. Barrio, and M. V. L. Bennett. 1993. Divergent properties of different connexins expressed in *Xenopus* oocytes. *In* Progress in Cell Research: Gap Junctions, Vol. 3. J. E. Hall, G. A. Zampighi, and R. M. Davis, editors. Elvesier, Amsterdam. 3–13.

Nicholson, B. J., L. Zhou, F. Cao, H. Zhiu, and Y. Chen. 1998. Diverse molecular mechanisms of gap junction channel gating. *In* Gap Junctions. R. Werner, editor. IOS Press, Amsterdam. 3–7.

Oh, S., Y. Ri, M. V. L. Bennett, E. B. Trexler, V. K. Verselis, and T. A. Bargiello. 1997. Changes in permeability caused by connexin 32 mutations underlie X-linked Charcot-Marie-Tooth disease. *Neuron.* 19:927–938.

Rabadan-Diehl, C., G. Dahl, and R. Werner. 1994. A connexin-32 mutation associated with Charcot-Marie-Tooth disease does not affect channel formation in oocytes. *FEBS Lett.* 351:90–94.

Sosinsky, G. E. 1992. Image analysis of gap junction structures. *Electron. Microsc. Rev.* 5:59–76.

Sosinsky, G. E. 1996. Molecular organization of gap junction membrane channels. *J. Bioenerg. Biomembr.* 28:297–310.

Spray, D. C., A. L. Harris, and M. V. L. Bennett. 1981. Equilibrium properties of a voltage-dependent junctional conductance. *J. Gen. Physiol.* 77:77–93.

Suckyna, T. M., L. Xian-Xu, F. Gao, C. R. Fourtner, and B. J. Nicholson. 1993. Identification of a proline residue as a transduction element involved in voltage gating of gap junctions. *Nature.* 365:847–849.

Unger, V. M., N. M. Kumar, N. B. Gilula, and M. Yeager. 1997. Projection structure of gap junction membrane channel at 7 197 Å resolution. *Nature Struct. Biol.* 4:39–43.

Unwin, P. N. T., and P. D. Ennis. 1984. Two configurations of a channel-forming protein. *Nature.* 307:609–613.

Unwin, P. N. T., and G. Zampighi. 1980. Structure of the junctions between communicating cells. *Nature.* 283:545–549.

Valiunas, V., F. F. Bukauskas, and R. Weingart. 1997. Conductances and selective permeability of connexin-43 gap junction channels examined in neonatal heart cells. *Circ. Res.* 80:708–719.

Verselis, V. K., C. S. Ginter, and T. A. Bargiello. 1994. Opposite voltage gating polarities of two closely related connexins. *Nature.* 368:348–351.

Wang, H.-Z., L. Li, F. Lemanski, and R. D. Veenstra. 1992. Gating of mammalian cardiac gap junction channels by transjunctional voltage. *Biophys. J.* 63:139–151.

White, T. W., R. Bruzzone, and D. L. Paul. 1995. The connexin family of intercellular channel forming proteins. *Kidney Int.* 48:1148–1157.

Wilders, R., and H. J. Jongsma. 1992. Limitations of the dual voltage clamp method in assaying conductance and kinetics of gap junction channels. *Biophys. J.* 63:942–953.

Willecke, K., R. Heynkes, E. Dahl, R. Stutenkemper, H. Hennemann, S. Jungbluth, T. Suchyna, and B. J. Nicholson. 1991. Mouse connexin37: cloning and functional expression of a gap junction gene highly expressed in lung. *J. Cell Biol.* 114:1049–1057.

Yancy, S. B., S. A. John, R. Lal, B. J. Austin, and J.-P. Revel. 1989. The 43-kD polypeptide of heart gap junctions: immunolocalization, topology, and functional domains. *J. Cell Biol.* 108:2241–2254.

Yeager, M., and N. B. Gilula. 1992. Membrane topology and quartenary structure of cardiac gap junction ion channels. *J. Mol. Biol.* 223:929–948.

Zimmer, D. B., C. R. Green, W. H. Evans, and N. B. Gilula. 1987. Topological analysis of the major protein in isolated intact rat liver gap junctions and gap junction-derivated single membrane structures. *J. Biol. Chem.* 262:7751–7763.